

# Toward the Combination of the Most Reliable Terrestrial and Satellite Gravimetric Data for Precise Geoid Determination of Egypt

Ahmed Shaker<sup>a</sup>, Abdallah Saad<sup>a</sup>, Abdelhameed Elharty<sup>a\*</sup>

<sup>a</sup> Geomatics Engineering Department, Faculty of Engineering at Shoubra, Benha University, Egypt.

\* Corresponding Author

E-mail: abdelhamid.muhammed@feng.bu.edu.eg, Abdallah.saad@feng.bu.edu.eg, a.shaker@feng.bu.edu.eg.

**Abstract:** . The gravity field is important to determine the size and shape of the earth, to determine the heights, to investigate the structure of the crust, and to explore the mineral wealth. A lot of gravity observations have been taken in Egypt. Those gravity observations are taken over a long-time span with different gravimeters, different references, and different processing methodologies. Those huge amounts of data need to be filtered and unified before using them in precise geoid determination. In the advent of satellite missions for gravity field determination and the yielded global gravity models with good resolution and precision, filtering the terrestrial observed gravity and improving the global gravity models should be done. In this research, the recent Global Geopotential Models (GGMs) will be used in filtering the terrestrial gravity anomalies, and then the reliable terrestrial anomalies will be used in improving the global model gravity anomalies. Four recent GGMs (EGM2008, XGM2019e\_2159, GOCO06s, and SGG-UGM 2) are validated using terrestrial gravity anomalies to determine which model best fits the Earth's external gravity field in Egypt. Thousands of terrestrial gravity anomalies are collected as different data sets, so one of the aims of this research is to unify them using the common points among them. Finally, gravity anomalies are used to obtain their corresponding undulation values using a simple model. The obtained results of this study are recommended when collecting all the gravity observations taken all over Egypt to compute precise gravimetric geoid.

**Keywords:** : Terrestrial gravity, GGMs validation, GGMs improving, Filtering, Unification.

## 1. INTRODUCTION

High-resolution gravity models can be derived from a combination of the gravity signals from satellite gravity data, satellite altimetry data, surface gravity data, airborne gravity data, shipborne gravity data, and terrain models [1]. The global models are either satellite-only or combined (terrestrial and satellite) models. It is now possible to represent the Earth's global gravity field and its variations with better spatial and temporal resolutions compared to the first-generation global gravity field models derived from the 1960s to 1990s due largely to the highly accurate satellite data measured by today's developing technology.

Earth's shape, its interior and fluid envelope, and mass change, which give hints to climate-related changes in the Earth system, may be provided by GGMs. The computation of gravity field functionals (e.g., geoid undulations, gravity

anomalies) from the model representation is, therefore, not only relevant for geodesy but also for other geosciences, such as geophysics, glaciology, hydrology, oceanography, and climatology [2]. Gravity is a regionalized field; since gravity varies gradually from place to place without providing for the correlation of a specific mathematical function. The technique that maintains both the fine and coarse properties of the original gravity data analyzed without adding excessive distortions is the most accurate one for predicting gravity anomalies [3].

Despite more locations and areas that do not have terrestrial gravity anomaly observations, which may be due to the inaccessibility of newly chosen gravity points or obstacles like the dense forests in the selectable area, gravity anomalies can be predicted for such stations. Previous studies discussed several techniques used in the estimation method, including classical least squares,

remove-restore', and advanced techniques like least squares collocation and fast Fourier transformation.

Many gravity observations have been taken in Egypt over the last century. Those gravity observations are taken through long-time span with different gravimeters, different references, different processing methodologies, and different accuracies. Those observations need to be filtered and unified before using them in precise geoid determination.

Four main steps are done in this research. Firstly, four recent global geoid models are evaluated using terrestrial gravity anomalies, and the best global model is adopted for the next computation steps. Secondly, the available terrestrial gravity anomalies in this research are refined by comparing them with their corresponding values from the adopted global geoid model, and odd values are rejected. Thirdly, the different data sets of gravity anomalies are then unified to the recent gravity network in Egypt using the common stations between those networks.

Finally, geoid undulations are computed from gravity anomalies using a simple mathematical model and employing some stations of known undulations and anomalies. So, this research includes four main steps:

1. Evaluation of global geopotential models.
2. Filtering the terrestrial gravity observations.
3. Improving the performance of the global models.
4. Predicting the undulations from the gravity anomalies.

## 2. USED DATA

### 2.1 Terrestrial gravity data

Five datasets of terrestrial free-air gravity anomaly stations are accessible. The BGI shared 3497 stations [4], Fugro Ground Geophysics (FGG) Company delivered [5]3929 stations (dataset2), and 2034 terrestrial gravity stations (dataset1) were provided for the public. Besides, two precise networks of ground data: (a) The National Gravity Standard Base Net of Egypt (NGSBN77) consists of 98 stations with standard deviations ranging from 0.01 to 0.18 mGal [6]. This network includes existing stations of the International Gravity Standardization Net 1971 (IGSN71) in Egypt (11 stations) [7]. (b) The Egyptian National Gravity Standardization Network of 1997 (ENGSN97) modified by SRI (Survey Research Institute), contains five absolute and 145 relative gravity stations covering Egypt with residuals ranging from -0.07 to 0.07 mgal [6]. The spatial distribution of all available terrestrial gravity anomaly stations is plotted in figure 1.

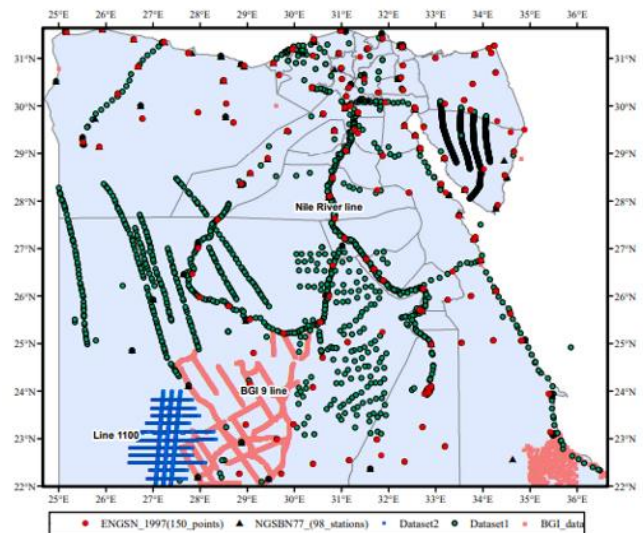


Fig 1. The available terrestrial gravity anomalies distributed in the study area (Egypt).

### 2.2 Global Gravitational Models (GGMs)

Another source of gravity data was the International Center for Global Earth Models (ICGEM) website, which is linked by [8]. This organization provided four GGMs which have been used in the study, and these models are:

- (i) XGM2019e\_2159 model, which was released in 2019, the data that have been used in this combining model are satellite altimetry data, terrestrial gravity data, and the GOCO06s model [9].
- (ii) GOCO06s is a recent satellite-only global gravity field model up to degree and order 300, and it has been provided by gravity observation data collected from 19 satellites over 15 years using various observation techniques [10].
- (iii) EGM2008 model was published in 2009 with degree and order 2159, and the model over areas covered with high-quality gravity data, the variations between the GNSS/Leveling results and the independent EGM2008 geoid undulations range from  $\pm 5$  to  $\pm 10$  cm [11].
- (iv) SGG-UGM 2 model was released in 2020 from satellite gravimetry data, satellite altimetry data, and EGM2008 data [3]. The highest resolution among all available models is about 2190 with respect to degree and order, depending on latitude. On the other hand, the accuracy of the model mainly depends on the type of quality and amount of data used for creating the GGMs [12].

The main attributes of these GGMs are shown in table 1. Also, in the data column of the table, the datasets used in the development of the models are summarized, where A is for altimetry, S is for satellite (e.g., GRACE, GOCE, LAGEOS), G for ground data (e.g., terrestrial, airborne, and

shipborne measurements). The GGMs used in the study were validated by several world organizations according to the Root mean square (RMS) of the differences between

GNSS leveling and quasi-geoid heights derived from GGMs. Statistics of this comparison are shown in table 2 (ICGEM, <http://icgem.gfz-potsdam.de/>).

**TABLE 1.** Main description of GGMs used in the research.

Model	Year	Degree	Data
SGG-UGM-2	2020	2190	A, S (GOCE, GRACE), EGM08
XGM2019e_2159	2019	2190	A, G, S(GOCO06s)
GOCO06s	2019	300	S
EGM 2008	2008	2190	A, G, S(Grace)

**TABLE 2.** RMS about the mean of GPS levelling minus gravity field model derived geoid heights, Unit in [m]

Model	Australia	Brazil	Canada	Europe	Japan	Mexico	USA	All
	No. of points have been used in the validation							
	7224	1154	2706	1047	816	4898	6169	24014
SGG-UGM-2	0.091	0.234	0.139	0.121	0.074	0.19	0.249	0.177
XGM2019e_2159	0.097	0.208	0.139	0.127	0.09	0.173	0.248	0.173
GOCO06s	0.259	0.32	0.297	0.341	0.43	0.346	0.398	0.334
EGM2008	0.095	0.302	0.14	0.125	0.083	0.212	0.248	0.188

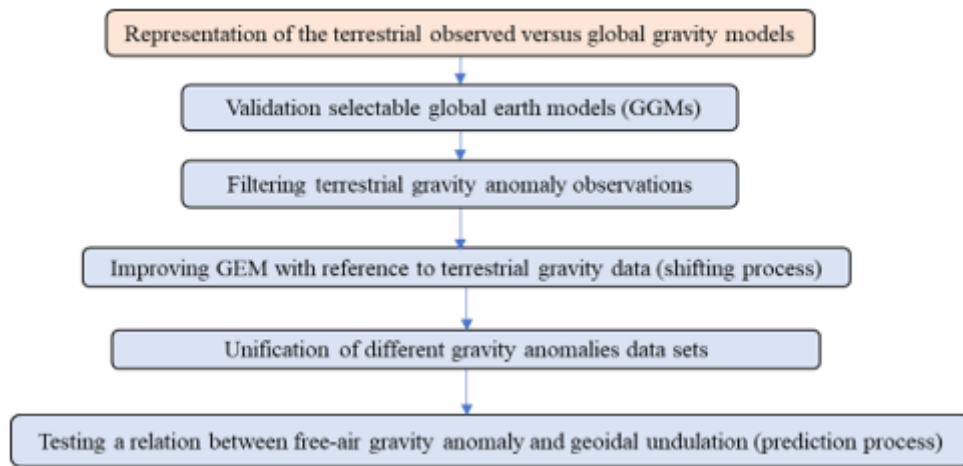


**Fig 2.** Main steps followed in the study.

### 3.1 GGMs Validation

The objective of this step is to evaluate some recent GGMs in the study area using terrestrial free-air gravity anomalies. Two types of GGMs are evaluated in this study: combined models (EGM2008, SGG-UGM-2, and XGM2019) and one satellite-only model (GOCO06s). To compare and analyze the performance of the different used global earth models to select the suitable one fitting the terrestrial data. The free-air anomalies from the models  $\Delta g_{FA(GEM)}$  were compared with their corresponding terrestrial observed values  $\Delta g_{FA(obs.)}$  and their differences  $\Delta(\Delta g_{FA})$  are expressed in terms of statistical parameters as:

$$\Delta(\Delta g_{FA}) = \Delta g_{FA(obs.)} - \Delta g_{FA(GEM)} \quad (1)$$

Validation of studied GGMs was done using 3 lines of terrestrial gravity anomalies gathered along the study area, as in figures 3 and 4. Firstly, the **Nile River line** of the

satellite gravity data was validated, and the minimum, maximum, mean, and Root Mean Squares (RMS) values of the differences between the two data sources were computed and tabulated for 93 stations along 366 km. From figure 3, the best model was found to be SGG-UGM 2 with 4.9 mGal RMS and 11.54 mGal as mean, but the largest RMS and mean were determined as 12.19, 15.4 mGal respectively for the satellite-only model (GOCO06s) which has degree and order of 300.

Secondly, the **line (BGI 9)** used to validate the same GGMs in the southwest desert of Egypt includes 95 points along 103 km. The relation between terrestrial and model anomalies for this line is obtained. Again, the results show that SGG-UGM 2 model is the best among the tested models.

Finally, **Line (1100)** contains 284 terrestrial observation points along 123 km, and the distance between

every successive two points is from 400 to 500 meters. Also, statistics results show that SGG-UGM2 global gravitational model has the best accuracy among the tested GGMs, its standard deviation and mean have been calculated as 2.856 and -2.3 mGal, respectively.

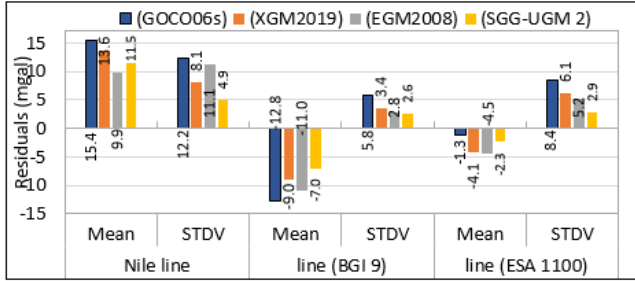


Fig 3. Statistics of the differences between the observed anomalies and their corresponding values from the global models for evaluated lines.

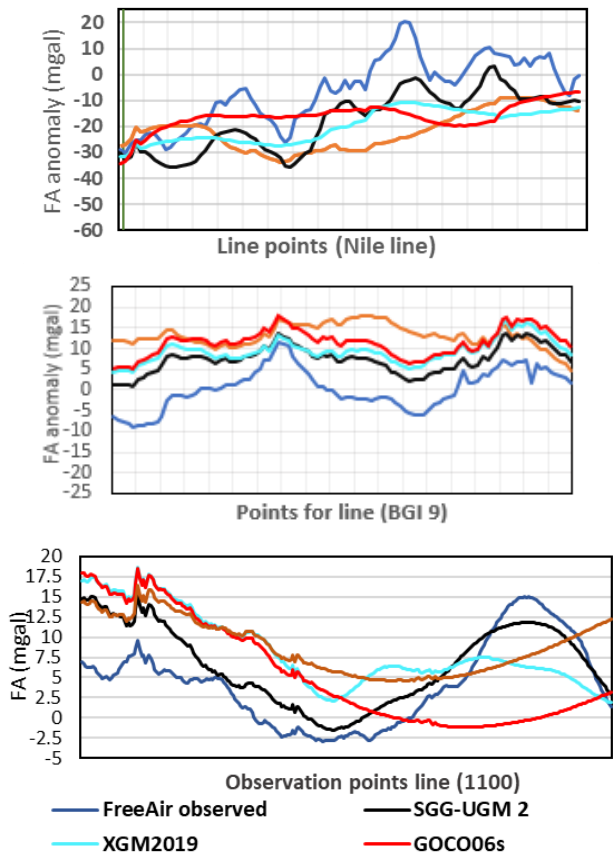


Fig 4. free air gravity anomalies of GGMs versus the terrestrial data for the evaluated lines: Nile line, BGI 9 line, and line (1100)

It can be noticed from the obtained results of the three test lines that SGG-UGM2 is the nearest tested GGMs to the terrestrial observations in the study area, so it will be employed in the computations of the rest of the research.

### 3.2 Filtering and Shifting Process.

In flat terrain areas like most of the data areas in this research, The local gravity field mostly changes smoothly. Filtering the observed gravity anomalies will be done here firstly by looking for sudden changes in the profile trend of the anomaly values, inconsistent value with the values around it. Secondly, to assure the first step, the anomaly values are compared with their corresponding values from the adopted global model (SGG-UGM 2), large differences compared to neighboring surrounding differences assure odd points.

After the filtering process is done, a shifting process is utilized to improve the performance of the used global model:

$$S = \Delta g(t)_{CP} - \Delta g(m)_{CP} \tag{2}$$

$$\Delta g(m)_{SH} = \Delta g(m) + S \tag{3}$$

Where:

- S is the shifted value between terrestrial ( $\Delta g(t)_{CP}$ ) and modeled ( $\Delta g(m)_{CP}$ ) anomaly shifted point.
- $\Delta g(m)_{SH}$  is the shifted free air gravity anomaly for the model.
- $\Delta g(m)$  is the free air gravity anomaly for the model.

The model line will be divided into sections, and the model anomalies will be shifted, using one terrestrial center point for every section. The shifted model values will be compared to the observed anomalies, and the differences will be tested.

For the Nile River line, figure (5) shows inconsistencies between observed and corresponding model anomalies at certain points. After excluding 16 odd points, out of 109 points, the RMS of the differences between the two anomaly sets reduced from 7.8 to 4.9 mGal. The range of the differences decreased from 43 to 22 mGal.

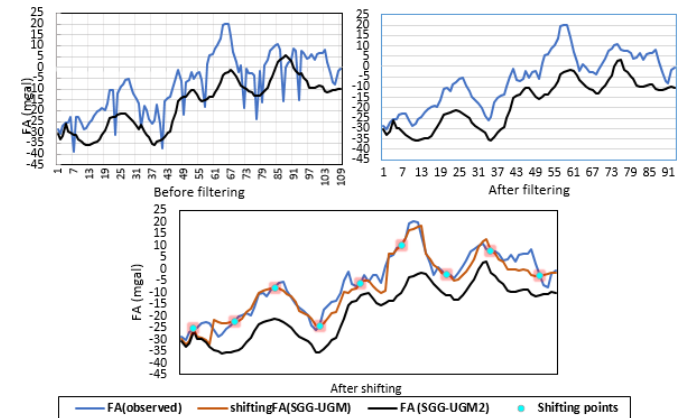


Fig 5. Observed Free Air gravity anomalies and their corresponding model values of the Nile line

The figure shows that the two lines of different data sources became more similar after rejecting the odd points and shows the consistency between the observed and

the model anomalies. It illustrates some constant shifts between the two profiles.

To improve the anomalies of the model, the shifting process is done every 40 km using nine terrestrial points, and the results are shown in table 3 and figure 5. The mean and standard deviation of the differences between observed and model anomalies are 11.55 and 4.90 mGal, while after shifting, they reduced to 1.5 and 3.57 mGal.

**TABLE 3.** Residuals between observed and corresponding model anomalies for different cases

Data (mGal)	Min	Max	Mean	STDV
FA (SGG-UGM 2 model)	-35.74	5.637	-16.95	11.90
Terrestrial free air anomaly	-38.63	20.24	-7.845	13.69
Residuals (observed – model)	-20.15	23.038	9.111	7.839
Filtered observed data	-30.38	20.242	-6.230	12.928
Residuals after filtering	0.910	23.038	11.545	4.903
Residuals after shifting the model	-6.109	10.839	1.516	3.572

**For Line (BGI 9)** in the southwest of Egypt, which includes 95 points along 103 km. Figure 6 obtains the changes of the data line before and after shifting the model data. The RMS and the mean of the differences between observed and shifted FA gravity anomalies are decreased from 2.6 to 1.75 mGal and from -6.95 to 1.36 mGal, respectively. Based on the obtained results, one can use the free available recent global model to obtain gravity anomalies and shifting them using some terrestrial anomalies instead of observing the whole required points. Nine instead of 93 points every 40 km in the Nile line have recorded 3.6 mgal standard deviation (STDV). On the other hand, 5 instead of 94 points every 20 km in the (BGI 9) line have recorded 1.75 mgal.

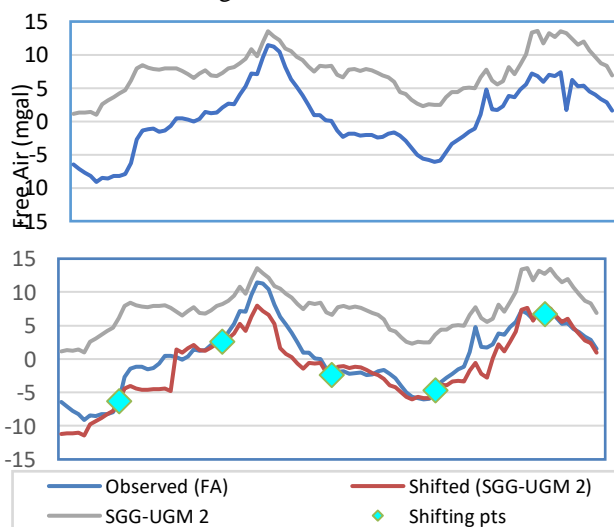


**Fig 6.** Observed and shifted model anomalies along line BGI 9

Filtering and shifting tests are done for 77 cases in Egypt, and similar results are obtained [13]. The results of the shifting process show that the RMS and mean of the differences between observed terrestrial FA gravity anomalies and the corresponding values from shifted FA gravity anomaly data model are improved by 27% : 34% and 80% : 86%, respectively compared to the data before shifting process.

**3.3 Unification of Different Gravity Anomalies Data Sets**

Gravity data in the study area have been collected by different institutions in different coordinate systems, different gravity base stations, and different vertical datums over many decades. Consequently, this research assesses the suitability of analyzing the available terrestrial gravity datasets (figure 1) and unifying the observation values for ensuring geoid modeling accuracy. The steps which have been followed in the unification process are discussed as:

Firstly, determining the same (common) stations in every two datasets, regarding that the horizontal positioning differences between WGS 84 and the Old Egyptian Datum reach about 200 meters all over Egypt [14]. Then to compute, as an example, the transformation parameters between the free air gravity anomaly values of ENGSN 1997 and NGSBN 77 datasets, parametric least squares adjustment has been done according to the assumed simple linear formula:

$$\Delta g_{FA(97)} = a_0 + a_1 * lat + a_2 * lon + a_3 \Delta g_{FA(77)} \quad (4)$$

Where:  $\Delta g_{FA(97)}$ ,  $\Delta g_{FA(77)}$  are free air gravity anomalies for ENGSN1997 and NGSBN 77,  $a_0, a_1, a_2, a_3$  are the unknown parameters.

Then lastly, the transformed values of the dataset have been obtained using the computed transformation parameters.

For the unification between ENGSN 1997 with NGSBN 77 (figure 1), it is found that 34 gravity stations are common between the two data sets. The unknown parameters of equation 4 have been calculated using 24 solution points and 9 points are used as check points, and the statistics of the differences between the free air anomaly of the two systems are computed before and after the unification as in tables (4) and (5).

**TABLE 4.** Statistics of the differences between the values of 1977 and their corresponding values of 1997

	Min	Max	Mean	STDV
(Net 97 - Net 77) at 24 solution points	-3.590	4.776	0.433	1.761
(Net 97 - Net 77) at 9 check points	-1.673	3.222	0.569	1.567

**TABLE 5.** Transformation parameters and statistics of the differences between transformed values of 1977 and their corresponding value of 1997

Transformation parameters	a0	a1	a2	a3
		-17.48	0.43	0.18
Units in mgal	Min	Max	Mean	STDV
Residuals at 24 solution points	-3.857	4.150	0.00	1.617
Residuals at 9 checkpoints	-3.675	2.348	-0.119	1.754

The previous steps are applied to unify dataset1 with ENGSN 1997. The common gravity observation points between the ENGSN97 and dataset1 are determined and analyzed.

The common points between the two datasets are 125 gravity observation points. The differences between the two observation sets are calculated and the statistics of the differences are determined as below:

**TABLE 6.** Statistics of the differences between the two observation sets (ENGSN97 and Dataset1).

Free air (in mgal)	Min	Max	Mean	STDV
Residuals	-6.12	5.57	-0.05	2.77

The transformation parameters between the two nets are computed over 39 common points and the rest of all common points are defined as checkpoints (86 common points) for the solution parameters. The transformed data is obtained, and the statistics of the results are determined, as shown in table 7.

**TABLE 7.** The statistics of the differences between the free air anomaly of ENGSN97 and Dataset1

Units in mgal	Min	Max	Mean	STDV
Residuals at 39 solution points	-3.94	4.60	0.00	2.20
Residuals at 86 checkpoints	-6.67	5.57	-0.78	2.83

After the parameters between ENGSN97 and Dataset1 have been determined, the free air gravity anomalies for 2029 observed stations of dataset1 have been transformed.

**4. Predicting Geoid Undulations from Free-Air Gravity Anomalies.**

An Earth geopotential model and a collection of precise local data are often used in gravimetric geoid modeling [15]. Instead, a simple prediction process is proposed to obtain the wanted and not available geoid undulations from the gravity anomalies that exist over the Egyptian territory, especially in desert areas. Geoid undulations (N) are needed in obtaining orthometric heights (H) from the GNSS ellipsoidal heights (h) as follows:

$$H = h - N \tag{5}$$

On the other hand, gravity anomaly ( $\Delta g$ ) is the difference between the gravity on the geoid ( $g_0$ ) and the normal ravity

on the ellipsoid ( $\gamma$ ), consequently, the free air gravity anomaly is obtained by applying the reduction of free air for the gravity observation point on the earth’s surface ( $g$ ) (equation 6), [16]. Furthermore, the simple assumed multiple linear regression equation is proposed to relate the geoid undulations(N)with the gravity anomalies ( $\Delta g$ )(equation 7).

$$\Delta g_{FA} = g + FA - \gamma \tag{6}$$

$$N = a_0 + a_1\varphi + a_2\lambda + a_3\Delta g \tag{7}$$

Where:  $FA$  is the free air reduction which equals to ( $FA = 0.3086 H$ ),  $N$  is the geoidal undulation in meters, ( $\varphi, \lambda$ ) are latitude and longitude at a point in decimal degrees,  $\Delta g$  refers to the Free-air gravity anomaly the point in mGal, and  $a_0, a_1, a_2,$  and  $a_3$  are the unknown coefficients of the equation. Note that  $N$  and  $\Delta g$  refer to the same point.

The equation is written at some well distributed stations (training points) along the data line using known undulations and anomalies to obtain the unknown coefficients for the whole line. Then those coefficients are applied at the whole points (test points) of the line to obtain predicted undulations from their corresponding anomalies. The predicted undulations are then compared to the original undulations, and the differences are analyzed. Different spacing distances between the solution points are tested to obtain the optimum case. The prediction process is applied to line data and for area data. To avoid any biases in the used data, the prediction process is carried out using undulations and anomalies of the global model, i.e the same data source, to avoid any observational errors and check only the proposed model. Then as a second step, it is carried out using actual observations.

**4.1. Prediction Using Global Model Data.**

Testing the predicted equation for the adopted global gravitational model (SGG-UGM2) using the free air gravity anomaly and the undulation of the model.

Firstly, six solution points (70 km between every two successive points), out of 93 test points of the Nile line are used to determine the unknown coefficients of the prediction formula (7) by the least squares method. The obtained results showed that the range, the mean, and the STDV of the differences between predicted and model undulations are from -0.17 to 0.29, 0.05, and 0.10m, respectively.

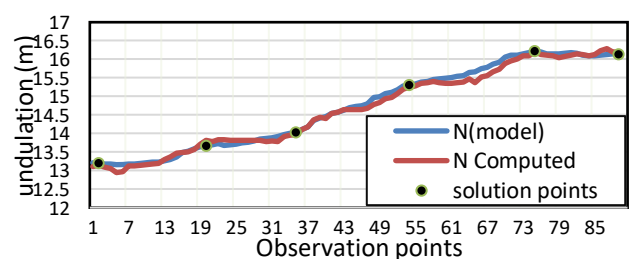


**Fig 7.** Predicted against model undulations, six solution points, along 342 km, Nile line.

The prediction process is repeated using eight solution points, with 50 km spacing between every two successive points. The range, the mean, and the STDV of the differences between computed and model undulations are from -0.25 to 0.37, 0.02, and 0.13m, respectively. This process can also be done for an area of data by:

- Firstly, the data area was treated with different radii from 10 to 70 km with the same center point for all cases, as in figure 8.
- Secondly, seven well distributed solution points have been assigned for each case
- Thirdly, using the assumed linear regression model, geoidal undulations of all observation stations have been computed. Finally, the statistical analysis of the differences between the observed and predicted values was determined in table (8), figure (9).

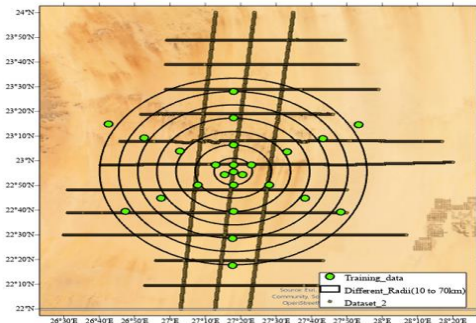


**Fig 8.** Dataset 2 ground data with different radii from 10 to 70 km and solution points.

**Table 8.** Statistics of the differences between original and corresponding predicted undulations

	Solution pts	Test points	Mean (m)	STDV (m)
Case 1 R=10 km	7	62	0.000	0.000
Case 2 R=20 km	7	222	0.006	0.013
Case 3 R=30 km	7	499	0.022	0.053
Case 4 R=40 km	7	844	0.007	0.047
Case 5 R=50 km	7	1311	0.016	0.042
Case 6 R=60 km	7	1741	-0.016	0.052
Case 7 R=70 km	7	2325	-0.013	0.056

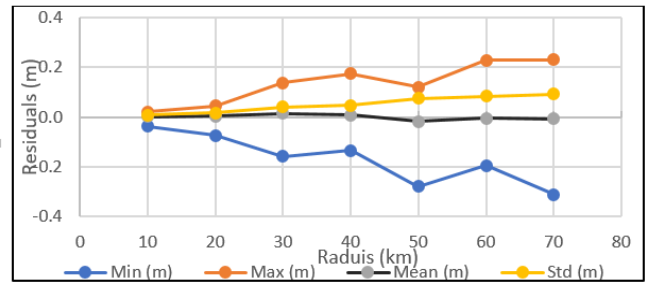


**Fig 9.** Statistics of the differences between predicted and model undulations, different radii used.

Seven solution points with known undulations and anomalies are used to predict the undulations at hundreds of points with known anomalies. As it is clear, the resulted mean and STDV of the differences are satisfactory for many applications.

**4.2. Prediction Using Observed GPS-Levelling Data.**

In the previous part, the predicted undulations from global model anomalies were compared with their corresponding original values from the model. The available data does not contain observed anomalies and observed undulations on the same points of the same data set. Observed anomalies along the Nile line on the **desert road** from Asyut to Helwan are available. On the other hand, observed undulations along the Nile River on the **agriculture road** are available too. The average distance between observed gravity points and observed undulation points ranges from 0.5 to 5 km, figure (10), the difference is neglected for approximate evaluation of the process.

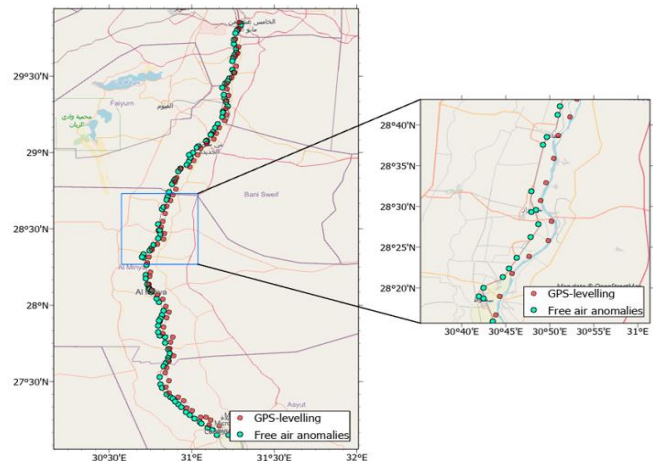


**Fig 10.** Observed free-air gravity anomalies and undulations near the Nile River line.

The differences between predicted and observed undulations, using eight training points, every 50 km are computed. The range, mean value, and the STDV of the results are from -0.199 to 0.26, -0.002, and 0.105 m, respectively figure (11). Regarding the

undulation values are not exactly at the anomaly points, the results are comparable with the data model case, and they are satisfactory for many applications, especially in distant desert areas.

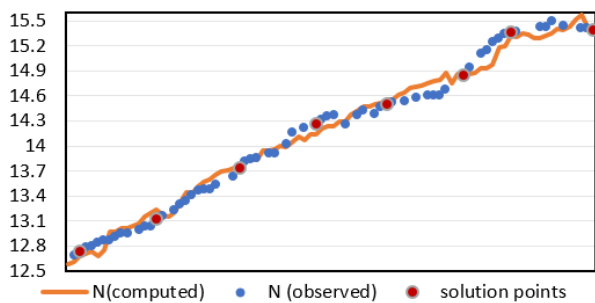


Fig 11. Predicted against observed undulations along the Nile line, using 8 points, every 50 km.

## 5. CONCLUSION

Firstly, the four global gravity models (EGM2008, SGG-UGM 2, XGM2019, and GOCO06s) are evaluated against terrestrial observed gravity anomalies at three different lines of data, so these lines have recorded the largest and smallest standard deviation for GOCO06s and SGG-UGM 2 model respectively. Consequently, SGG-UGM 2 is adapted to be used in the computations in this research.

Secondly, Odd terrestrial gravity anomalies were filtered by comparing them with their corresponding values from the adopted model. Sudden changes in the observed gravity anomalies have been rejected. Then the terrestrial anomalies became more consistent than before. Thirdly, the gravity anomalies of the adopted model are shifted using some observed terrestrial anomalies. The shifted model values are then examined against the observed values. The shifting process improved the performance of the global model. Besides, it saves money, time, and effort where one can observe some points and use them in shifting the released global model to obtain better anomalies around them with a radius exceeding 40 km.

Finally, geoid undulations are obtained from the available gravity anomalies through simple linear relations. Some observed undulations are needed along a line data or an area data to change big number of observed gravity anomalies into corresponding undulations.

## ACKNOWLEDGMENTS

The authors thank the Bureau Gravimetric International (BGI) for providing terrestrial gravity data over the study area. The International Center for Global Gravity Field Models (ICGEM) is appreciated for making global gravity models available free of charge on its web page.

## REFERENCES

- [1]. Liang, W., Li, J., Xu, X., Zhang, S., and Zhao, Y., 2020. A High-Resolution Earth's Gravity Field Model SGG-UGM-2 from GOCE, GRACE, Satellite Altimetry, and EGM2008. *Engineering* 6(8), 860-878.
- [2]. Ince, E. S., Barthelmes, F., Reißland, S., Elger, K., Förste, C., Flechtner, F., and Schuh, H., 2019. ICGEM -15 years of successful collection and distribution of global gravitational models, associated services, and future plans. *Earth System Science Data*, 11, 647-674.
- [3]. Kamguia, J., Tabod, C., Tadjou, J. M., And Houetchak L. K., (2007): Accurate Gravity Anomaly Interpolation: A Case-Study In Camerron, Central Africa. *Earth Sciences Research Journal*, Vol. 11(2), 115-123.
- [4]. Bonvalot, S. and BGI team. International Gravimetric Bureau, created in 1951 by the International Association of Geodesy (IAGG) <<https://bgi.obs-mip.fr/fr/francais/>>
- [5]. <https://www.fugro.com/our-services/land-site-characterisation/geological-and-geophysical-surveys>
- [6]. Dawod, G., Alnaggar, D. S., 2007. Quality Control Measures For The Egyptian National Gravity Standardization Network (ENGSN97), Proceedings of The Second International Conference on Civil Engineering, Helwan University.
- [7]. Gad, M. A., Odalovic, O., and Naod, S., 2020: Possibility to Determine Highly Precise Geoid for Egypt Territory, *Geodetski Vestnik*, Vol. 64(4), 578-593.
- [8]. Ince, E. S., Barthelmes, F. 2018, International Centre for Global Earth Models (ICGEM), accessed 20 February 2021, <<http://icgem.gfz-potsdam.de/>>
- [9]. Zingerle, P., Pail, R., Gruber, T., and Oikonomidou, X., 2020. The combined global gravity field model XGM2019e. *Journal of Geodesy*, vol. 94(66).
- [10]. Kvas, A., Brockmann, J. M., Krauss, S., Schubert, T., Gruber, T., Meyer, U., Gürr, T. M., Schuh, W. D., Jäggi, A., and Pail, R., 2021. The satellite-only gravity field model GOCO06s. *Earth System Science Data*, vol. 13(1), 99-118.
- [11]. Pavlis, N. K., Holmes, S. A., Kenyon, S. C., and Factor, J K.,(2012): The development and evaluation of the Earth Gravitational Model 2008 (EGM2008), *Journal of Geophysical Research: Solid Earth*.
- [12]. Alcantar-Elizondo, N., Garcia-Lopez, R. V., Torres-Carillo, X. G., Vazquez-Becerra, G. E., 2021. Combining Global Geopotential Models, Digital Elevation Models, and GNSS/Leveling for Precise Local Geoid Determination in Some Mexico Urban Areas: Case Study. *ISPRS International Journal of Geo-Information*, Vol. 10(12), 819.
- [13]. Elharty, A. (2023), Improving, filtering, and Predicting Gravity Field over Egypt using Terrestrial Gravity Data and Global Geopotential Models. Unpublished Master Thesis, Geomatics Department, Faculty of Engineering at Shoubra, Benha University, Egypt.
- [14]. Saad, A., and Saad, M., 2007. Simple Model for Improving the Accuracy of the Egyptian Geodetic Triangulation Network, FIG Working Week conference in Hong Kong SAR, China 13-17
- [15]. Gad, M. A., Odalović, O., Abdel-hey A., 2018. An assessment and enhancement of the newly geopotential models over Egypt territory. *International Journal of Scientific and Engineering Research*
- [16]. Hofmann-Wellenhof, B. and Moritz, H. (2005). *Physical Geodesy*. Berlin: Springer Verlag.